Available online at www.sciencedirect.com
ScienceDirect
Journal of Sound and Vibration 324 (2009) 161–178
JOURNAL OF SOUND AND VIBRATION
www.elsevier.com/locate/jsvi

Component mode synthesis as a framework for uncertainty analysis

L. Hinke, F. Dohnal, B.R. Mace*, T.P. Waters, N.S. Ferguson

Institute of Sound and Vibration Research, University of Southampton, Highfield, Southampton SO17 1BJ, UK

Received 6 June 2008; received in revised form 28 January 2009; accepted 29 January 2009
Handling Editor: C.L. Morfey
Available online 20 March 2009

Abstract

Component mode synthesis (CMS) is a well-established technique for the vibration analysis of built-up structures. It was originally developed as a method for reducing the size of a finite element model, hence reducing computational cost. CMS also offers an appealing framework for the analysis of the dynamics of uncertain structures. The benefits concern the numerical costs, the way uncertainty is included, quantified and propagated. This paper reviews and discusses these issues. The fixed-interface (Craig–Bampton) method is described, while the number of interface degrees of freedom (dofs) can be further reduced using characteristic constraint modes. Quantification and propagation of uncertainty is discussed. Uncertainties in properties can be naturally and straightforwardly introduced at the component level, either in terms of the component physical properties or the component modal properties, while the individual components are typically statistically independent, being made by different manufacturing processes. CMS methods are also amenable to the inclusion of experimentally measured variability data, quantifying it in terms of component modal properties. An example is given. The application of perturbational techniques is considered. The CMS framework is particularly amenable to propagation of uncertainty through one or more of the analysis paths at component or at global level using perturbations. Finally, qualitatively different uncertainty descriptions can be combined, with some components being described probabilistically, some possibilistically, the descriptions then being unified at the global level. Numerical examples are presented. Overall, CMS methods offer a strong physical insight into the analysis of structures with non-deterministic properties.

1. Introduction

The vibrations of mechanical structures are often analysed using the finite element (FE) method [1], where a deterministic model with one particular set of physical parameters is considered. However, the underlying assumption that the input data is precisely known is in general not valid, because there are uncertainties about the parameters, often until the last stage of the design cycle and even when the product is in service. Furthermore, every manufacturing process naturally and inevitably introduces some product variability. In this context, it is often more important to predict the variation in the response than attempt to improve further

*Corresponding author. Tel.: +44 23 8059 2344; fax: +44 23 8059 3190.
E-mail address: brm@isvr.soton.ac.uk (B.R. Mace).

0022-460X/$ - see front matter
doi:10.1016/j.jsv.2009.01.056

the accuracy of a deterministic model. The variation in input and response parameters can be described possibilistically [2], giving an envelope to all possible parameter values, or probabilistically [3], which also includes information on their probability of occurrence.

A promising methodology to address several of the challenges in the modelling of the dynamics of non-deterministic properties in complex structures is substructuring. Component mode synthesis (CMS) [4–7] methods are useful for the analysis of structures that are built-up of several components, as is generally the case in industrial applications. The components are modelled individually and their dynamic models are assembled to produce a much smaller model of the whole structure. In the analysis of structures with uncertain properties, a deterministic problem often has to be solved repeatedly, which is numerically expensive. In this context, deterministic model reduction by CMS is especially important because the benefits accrue multiple times.

There are further benefits, however. First, the individual components are typically statistically independent, being made up by different manufacturing processes, and so too are the joints. Reanalysis is required of only those elements of the structure which are uncertain, together with the (relatively small) global eigensolution. The second group of benefits concerns how uncertain data is quantified and included. Uncertainties in properties can be naturally and straightforwardly introduced at the component level, either in terms of the component physical properties or the component modal properties. The former typically requires quantification of a random field for each physical property, while the latter involves component natural frequencies—a discrete set of data of low order—and eigenfunctions. This enables possibilities for substantial reduction in the quantity of uncertain data that must be included in the model. Furthermore, it is potentially easier in practice to measure the variation in modal properties of a component, using a simple hammer test for example, than to quantify the spatial distribution of physical properties. Thirdly, CMS is suitable for both probabilistic and possibilistic uncertainty description and propagation, although the emphasis here is on probabilistic [2] and perturbational approaches [8]. Previous work concerning possibilistic methods includes that of De Gersem et al. [9], who considered the application of interval FE in CMS and suggested three schemes to reduce computational cost, these involving different levels of approximation. Giannini and Hanns [10] developed a component mode transformation method for the propagation of fuzzy parameters through a CMS model. Finally, advantages arise from the fact that each substructure can be treated independently regarding the quantification and propagation of non-deterministic data. For example, a hybrid description can be adopted, with different parts of a built-up structure perhaps being described by possibilistic and probabilistic concepts.

In this paper uncertainty modelling within the framework provided by CMS is discussed. Numerical models are most easily constructed using the fixed-interface (Craig–Bampton) method [5], while the number of interface degrees of freedom (dofs) can be further reduced by a decomposition into characteristic constraint (CC) modes [11]. These methods are reviewed in the next section. In Section 3 uncertainty quantification and propagation are discussed, with particular emphasis placed on perturbation methods. Illustrative examples are presented in Section 4. This is followed by a discussion and concluding remarks.

2. Fixed-interface CMS and CC modes

CMS was introduced in the 1960s by Hurty [4] and Craig and Bampton [5]. Reviews of CMS methods can be found in Refs. [6,7]. In CMS, models of each substructure are developed and assembled, together with models for the joints. The individual substructure models are transformed from physical to component modal coordinates, using a set of chosen basis functions. There are many possible choices for these basis functions [4–7], including normal modes, found from solving a component eigenvalue problem, and static constraint or attachment modes. The models are assembled and the global eigenvalue problem of the whole structure is solved. A reduction in size can be achieved by truncating both the component and the global modes. Further reductions in the number of interface dofs can also be achieved. This work will focus on the fixed-interface Craig–Bampton method [5] with CC modes [11].

2.1. Component analysis: fixed-interface normal modes and constraint modes

The equation of motion of component α, neglecting damping, is

$$\mathbf{m}^{\alpha}\ddot{\mathbf{u}}^{\alpha} + \mathbf{k}^{\alpha}\mathbf{u}^{\alpha} = \mathbf{f}^{\alpha} \tag{1}$$

where $\mathbf{u}^{\alpha}$ is the physical dofs, $\mathbf{f}^{\alpha}$ the corresponding forces and $\mathbf{m}^{\alpha}$ and $\mathbf{k}^{\alpha}$ are the mass and stiffness matrices of the component, respectively. Henceforth in this subsection the superscript α will be suppressed for clarity. The physical dofs can be partitioned into a set of interior dofs $\mathbf{u}_I$ and a set of interface, or boundary, dofs $\mathbf{u}_B$. Eq. (1) can be written as

$$\begin{bmatrix} \mathbf{m}_{II} & \mathbf{m}_{IB} \\ \mathbf{m}_{BI} & \mathbf{m}_{BB} \end{bmatrix} \begin{bmatrix} \ddot{\mathbf{u}}_I \\ \ddot{\mathbf{u}}_B \end{bmatrix} + \begin{bmatrix} \mathbf{k}_{II} & \mathbf{k}_{IB} \\ \mathbf{k}_{BI} & \mathbf{k}_{BB} \end{bmatrix} \begin{bmatrix} \mathbf{u}_I \\ \mathbf{u}_B \end{bmatrix} = \begin{bmatrix} \mathbf{f}_I \\ \mathbf{f}_B \end{bmatrix} \tag{2}$$

where $\mathbf{f}_B = 0$ if the interface is free and $\mathbf{u}_B = 0$ if the interface is fixed.

2.1.1. Fixed-interface normal modes

The fixed-interface normal modes of a component are the (mass normalised) eigenvectors of the component with the interface dofs fixed. The size of this eigenvalue problem equals the number of interior dofs. This eigenvalue problem is given by

$$(\mathbf{k}_{II} - \lambda_j^{fi}\mathbf{m}_{II})\boldsymbol{\phi}_{I,j} = \mathbf{0} \tag{3}$$

where λ_j^{fi} are the fixed-interface eigenvalues. The eigenvectors $\boldsymbol{\phi}_{I,j}$ form the columns of the fixed-interface modal matrix $\boldsymbol{\Phi}_I$. A subset of k modes are kept, reducing the size of the component model. The normal mode matrix is then

$$\boldsymbol{\Phi}_k = \begin{bmatrix} \boldsymbol{\Phi}_{Ik} \\ \mathbf{0}_{Bk} \end{bmatrix} \tag{4}$$

where $\mathbf{0}$ is a null matrix of appropriate size.

2.1.2. Constraint modes

A constraint mode is the static displacement of the component due to a unit displacement of one interface dof and with all other interface dofs fixed. This can be written in matrix form as

$$\begin{bmatrix} \mathbf{k}_{II} & \mathbf{k}_{IB} \\ \mathbf{k}_{BI} & \mathbf{k}_{BB} \end{bmatrix} \begin{bmatrix} \boldsymbol{\Psi}_{IB} \\ \mathbf{I}_{BB} \end{bmatrix} = \begin{bmatrix} \mathbf{0}_{IB} \\ \mathbf{R}_{BB} \end{bmatrix} \tag{5}$$

where $\boldsymbol{\Psi}_{IB}$ is a matrix of displacements of the interior dofs and $\mathbf{I}_{BB}$ is an identity matrix. $\mathbf{R}_{BB}$ are the forces at the interface nodes. The constraint mode matrix is

$$\boldsymbol{\Psi}_c = \begin{bmatrix} \boldsymbol{\Psi}_{IB} \\ \mathbf{I}_{BB} \end{bmatrix} = \begin{bmatrix} -\mathbf{k}_{II}^{-1}\mathbf{k}_{IB} \\ \mathbf{I}_{BB} \end{bmatrix} \tag{6}$$

2.1.3. Component modal space

In the fixed-interface CMS method, the component modal space comprises the kept fixed-interface normal modes $\boldsymbol{\Phi}_k$ and static constraint modes $\boldsymbol{\Psi}_c$, which are combined to give the component modal matrix

$$\mathbf{B} = [\boldsymbol{\Phi}_k \;\; \boldsymbol{\Psi}_c] \tag{7}$$

The constraint modes assure compatibility of displacements of the components at the interfaces, improve convergence and also yield the exact static solution. The transformation from physical coordinates $\mathbf{u}$ to component modal coordinates $\mathbf{q}$ is given by

$$\mathbf{u} = \begin{bmatrix} \mathbf{u}_I \\ \mathbf{u}_B \end{bmatrix} = \mathbf{Bq} = [\boldsymbol{\Phi}_k \quad \boldsymbol{\Psi}_c] \begin{bmatrix} \mathbf{q}_k \\ \mathbf{q}_c \end{bmatrix} = \begin{bmatrix} \boldsymbol{\Phi}_{Ik} & -\mathbf{k}_{II}^{-1}\mathbf{k}_{IB} \\ \mathbf{0} & \mathbf{I}_{BB} \end{bmatrix} \begin{bmatrix} \mathbf{q}_k \\ \mathbf{q}_c \end{bmatrix} \tag{8}$$

The interior physical coordinates $\mathbf{u}_I$ are transformed into the fixed-interface modal coordinates $\mathbf{q}_k$. The physical interface coordinates $\mathbf{u}_B$ are retained, but will be denoted as constraint coordinates $\mathbf{q}_c$. The component modal mass and stiffness matrices $\boldsymbol{\mu} = \mathbf{B}^{\mathrm{T}}\mathbf{mB}$, $\boldsymbol{\kappa} = \mathbf{B}^{\mathrm{T}}\mathbf{kB}$ have the form

$$\boldsymbol{\mu} = \begin{bmatrix} \mathbf{I}_{kk} & \mathbf{m}_{kc} \\ \mathbf{m}_{kc}^T & \mathbf{m}_{cc} \end{bmatrix}, \quad \boldsymbol{\kappa} = \begin{bmatrix} \boldsymbol{\Lambda}_{kk} & \mathbf{0} \\ \mathbf{0} & \mathbf{k}_{cc} \end{bmatrix} \tag{9}$$

The matrices $\mathbf{m}_{cc}$ and $\mathbf{k}_{cc}$ are the constraint modal mass and stiffness matrices for component α, $\mathbf{m}_{kc}$ is a coupling matrix and $\boldsymbol{\Lambda}_{kk}$ is a diagonal matrix of kept fixed-interface modal eigenvalues. The equation of motion for component α thus becomes

$$\boldsymbol{\mu}^{\alpha}\ddot{\mathbf{q}}^{\alpha} + \boldsymbol{\kappa}^{\alpha}\mathbf{q}^{\alpha} = \mathbf{f}_q^{\alpha}, \quad \mathbf{f}_q^{\alpha} = \mathbf{B}^{\alpha^{\mathrm{T}}}\mathbf{f}^{\alpha} \tag{10}$$

2.2. Synthesis of components

Consider the synthesis of two components denoted by α and β. Continuity of displacements at their common interface, given by $\mathbf{u}_B^{\alpha} = \mathbf{u}_B^{\beta}$, is transformed into the component modal space by Eq. (8) to become $\mathbf{q}_c^{\alpha} = \mathbf{q}_c^{\beta}$. A transformation matrix $\mathbf{C}$ to impose the coupling conditions is such that

$$\mathbf{q} = \begin{bmatrix} \mathbf{q}_k^{\alpha} \\ \mathbf{q}_c^{\alpha} \\ \mathbf{q}_k^{\beta} \\ \mathbf{q}_c^{\beta} \end{bmatrix} = \begin{bmatrix} \mathbf{I} & \mathbf{0} & \mathbf{0} \\ \mathbf{0} & \mathbf{0} & \mathbf{I} \\ \mathbf{0} & \mathbf{I} & \mathbf{0} \\ \mathbf{0} & \mathbf{0} & \mathbf{I} \end{bmatrix} \begin{bmatrix} \mathbf{q}_k^{\alpha} \\ \mathbf{q}_k^{\beta} \\ \mathbf{q}_c \end{bmatrix} = \mathbf{C} \begin{bmatrix} \mathbf{q}_k^{\alpha} \\ \mathbf{q}_k^{\beta} \\ \mathbf{q}_c \end{bmatrix} \tag{11}$$

At this stage the interface (constraint) coordinates $\mathbf{q}_c$ are augmented by any internal dofs in the joints. The component modal matrices are assembled based on Eq. (10) and the global mass and stiffness matrices become

$$\mathbf{M} = \begin{bmatrix} \mathbf{I}_{kk}^{\alpha} & \mathbf{0} & \mathbf{m}_{kc}^{\alpha} \\ \mathbf{0} & \mathbf{I}_{kk}^{\beta} & \mathbf{m}_{kc}^{\beta} \\ \mathbf{m}_{kc}^{\alpha\mathrm{T}} & \mathbf{m}_{kc}^{\beta\mathrm{T}} & \mathbf{M}_{cc} \end{bmatrix} \quad \mathbf{K} = \begin{bmatrix} \boldsymbol{\Lambda}_{kk}^{\alpha} & \mathbf{0} & \mathbf{0} \\ \mathbf{0} & \boldsymbol{\Lambda}_{kk}^{\beta} & \mathbf{0} \\ \mathbf{0} & \mathbf{0} & \mathbf{K}_{cc} \end{bmatrix} \tag{12}$$

where

$$\mathbf{M}_{cc} = \mathbf{m}_{cc}^{\alpha} + \mathbf{m}_{cc}^{\beta}, \quad \mathbf{K}_{cc} = \mathbf{k}_{cc}^{\alpha} + \mathbf{k}_{cc}^{\beta} \tag{13}$$

are augmented if appropriate by contributions from any internal joint dofs. Due to the simplicity of the transformation matrix $\mathbf{C}$, component synthesis is straightforward and the system matrices have the same structure as the component matrices. The global matrices are reduced in size based on the number of fixed-interface modes kept in the component mode matrices $\mathbf{B}^{\alpha}$ and $\mathbf{B}^{\beta}$.

2.3. Interface dof reduction—CC modes

There may be many interface dofs, especially in applications involving line and surface coupling. Consequently it might be desirable to reduce the number of interface dofs and various approaches have been proposed [11–16]. In Refs. [12,13] a set of interface modes was defined as the normal modes of the whole structure after performing a static condensation of the interface dofs. A truncation of this set of interface modes amounts to replacing the constraint modes by only the first few interface modes. The technique was further extended to free-interface and hybrid-interface CMS models in Ref. [16]. However, because the set of interface modes, by this definition, depends on the properties of the whole structure, the substructures are no longer independent as in classical CMS methods. Finally, in Ref. [15] the component coupling conditions are treated as generalised kinematic (for displacement) or natural (for force) boundary conditions by appending all the component models in a single vector. A concept of generalised interface dofs is then introduced as a basis for projection of the interface dofs.

A more appealing approach, perhaps, is the use of CC modes [11], and this is the approach adopted here. Eigenanalysis is performed on the partitions of the CMS mass and stiffness matrices $\mathbf{M}$ and $\mathbf{K}$ in Eq. (12) that correspond to the constraint modes. The resultant eigenvectors are referred to as CC modes, and their number is then reduced. The calculation and selection of CC modes is essentially a further modal analysis, although for a problem of limited size.

The CC modes [11] are the solutions to the eigenproblem

$$[\mathbf{K}_{cc} - \lambda_j \mathbf{M}_{cc}]\boldsymbol{\xi}_j = \mathbf{0} \tag{14}$$

The interface coordinates $\mathbf{q}_c$ are then projected onto the CC modes through the transformation

$$\mathbf{q}_c = \boldsymbol{\Xi}\mathbf{p}_c, \quad \boldsymbol{\Xi} = [\boldsymbol{\xi}_1 \;\; \boldsymbol{\xi}_2 \;\; \ldots \;\; \boldsymbol{\xi}_{n_c}] \tag{15}$$

where a reduction is obtained because only n_c CC modes are kept.

2.4. The global eigenproblem

The equation of motion of the global system is given by

$$\mathbf{M}^{gl}\ddot{\mathbf{p}} + \mathbf{K}^{gl}\mathbf{p} = \mathbf{F} \tag{16}$$

where

$$\mathbf{M}^{gl} = \begin{bmatrix} \mathbf{I}^{\alpha}_{kk} & \mathbf{0} & \tilde{\mathbf{m}}^{\alpha}_{kc} \\ \mathbf{0} & \mathbf{I}^{\beta}_{kk} & \tilde{\mathbf{m}}^{\beta}_{kc} \\ \tilde{\mathbf{m}}^{\alpha\mathrm{T}}_{kc} & \tilde{\mathbf{m}}^{\beta\mathrm{T}}_{kc} & \mathbf{I}_{cc} \end{bmatrix}, \quad \mathbf{K}^{gl} = \begin{bmatrix} \boldsymbol{\Lambda}^{\alpha}_{kk} & \mathbf{0} & \mathbf{0} \\ \mathbf{0} & \boldsymbol{\Lambda}^{\beta}_{kk} & \mathbf{0} \\ \mathbf{0} & \mathbf{0} & \boldsymbol{\Lambda}_{cc} \end{bmatrix}, \quad \mathbf{p} = \begin{bmatrix} \mathbf{q}^{\alpha}_{k} \\ \mathbf{q}^{\beta}_{k} \\ \mathbf{p}_c \end{bmatrix}$$

$$\mathbf{I}_{cc} = \boldsymbol{\Xi}^{\mathrm{T}}\mathbf{M}_{cc}\boldsymbol{\Xi}, \quad \boldsymbol{\Lambda}_{cc} = \boldsymbol{\Xi}^{\mathrm{T}}\mathbf{K}_{cc}\boldsymbol{\Xi}, \quad \tilde{\mathbf{m}}^{\alpha}_{kc} = \mathbf{m}^{\alpha}_{kc}\boldsymbol{\Xi} \tag{17}$$

Note that the CC mass and stiffness matrices are diagonal, with off-diagonal terms only appearing in the global mass matrix. The global eigenvalues λ_i^{gl} and eigenvectors $\boldsymbol{\phi}_i^{gl}$ are found from the eigenvalue problem

$$(\mathbf{K}^{gl} - \lambda_i^{gl}\mathbf{M}^{gl})\boldsymbol{\phi}_i^{gl} = \mathbf{0} \tag{18}$$

The transformation into global modal coordinates $\mathbf{y}$ is given by

$$\mathbf{p} = \boldsymbol{\Phi}\mathbf{y} \tag{19}$$

where $\boldsymbol{\Phi}$ is the matrix of global eigenvectors.

Note that in the reduction leading to Eq. (17) only certain component modes are kept. As a guideline, these should be all modes with natural frequencies less than (say) twice the highest frequency of interest. However, if there is large uncertainty in parameters this reduced basis might be inadequate. A more robust technique, such as the dynamic condensation technique proposed by Guedri et al. [17] might then be used.

3. Uncertainty and CMS: quantification and propagation

There are four different coordinate systems in the CMS framework as shown in Fig. 1: component and global, physical and modal. Uncertainty propagates through these and can be quantified in various ways.

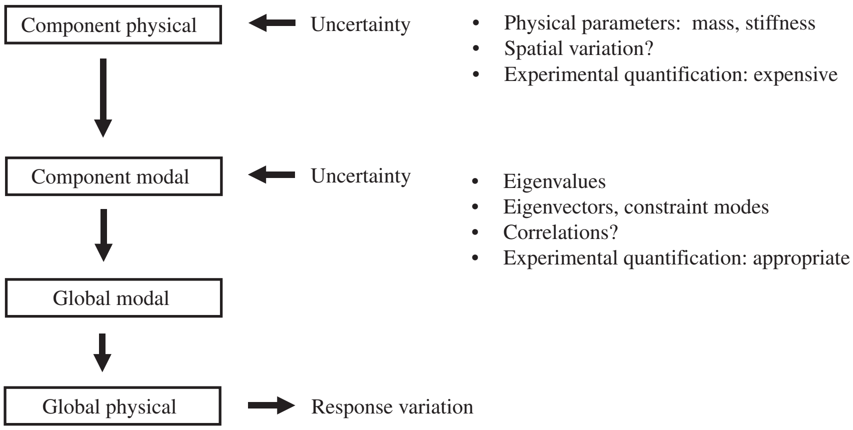

Fig. 1. Outline of uncertainty quantification in CMS.

3.1. Uncertainty quantification

Quantification of uncertainty is, in practice, a daunting task, and one that is often overlooked by the analyst. Only a very limited amount of measured data might be available and the quantification process, whether probabilistic or possibilistic, is likely to introduce substantial errors and approximations.

In principle, parametric uncertainties can be introduced at the physical level in terms of the mass and stiffness properties of individual components and the joints that connect them. In practice, many of these properties (thickness, elastic modulus, etc.) vary spatially and could be described by random fields [18]. However, quantification is difficult or even impossible, due to the effort and expense of acquiring data such as the correlation function or length of a random field. In most cases, experimental quantification at the physical level is difficult and expensive. Quantification in a numerical model is therefore an approximation.

CMS models offer an alternative, that of introducing uncertainties at the component modal level in terms of the modal parameters: the fixed-interface component eigenfrequencies, mode shapes, constraint modes and perhaps CC modes. The special structure of the global matrices (Eq. (12) or (17)), where the component eigenvalues appear uncoupled on the diagonal of the stiffness matrix, is advantageous for this purpose.

Experimental quantification of the eigenvalues and their statistics is straightforward using simple hammer tests, for example, on an ensemble of structures. In practice it might be simplest to perform this with a free rather than fixed interface, although one can estimate the statistics of the latter from those of the former [19]. The quantification of uncertainty in the mode shapes and in the constraint terms is not so straightforward, however, although there are reasons to suppose that the response statistics are less sensitive to these (see below). A simple and practical approximate approach is therefore to consider variation in component eigenfrequencies only. The inaccuracies and errors caused by this approach will be investigated later. In contrast to physical properties, quantification in modal properties takes account of all sources of uncertainty, including non-parametric effects. Finally it should be noted that it is possible to describe uncertainty in different subsystems in qualitatively different manners, some possibilistically and some probabilistically.

3.1.1. Example: natural frequency statistics of alloy wheels

As an illustrative example, consider the natural frequencies of a freely suspended alloy wheel such as that shown in Fig. 2(a). These frequencies affect the tyre/road noise. Each wheel is cast and then machined to final form. Differences arise from a variety of sources, including inclusions created during the casting process, different tempering times and temperature, slight differences in the properties of the alloy from one product run to another and tolerancing differences between CNC workstations. The lowest four natural frequencies of 79 nominally identical wheel rims were measured using a hammer test [20]. Their distributions were more-or-less Gaussian, with occasional outliers. The normalised variance and range were typically 0.5 and 3 percent, respectively. There was some correlation between the first and second natural frequencies, but little between any others (see Figs. 2(b) and (c)). To a good approximation, then, they can be assumed in any modelling

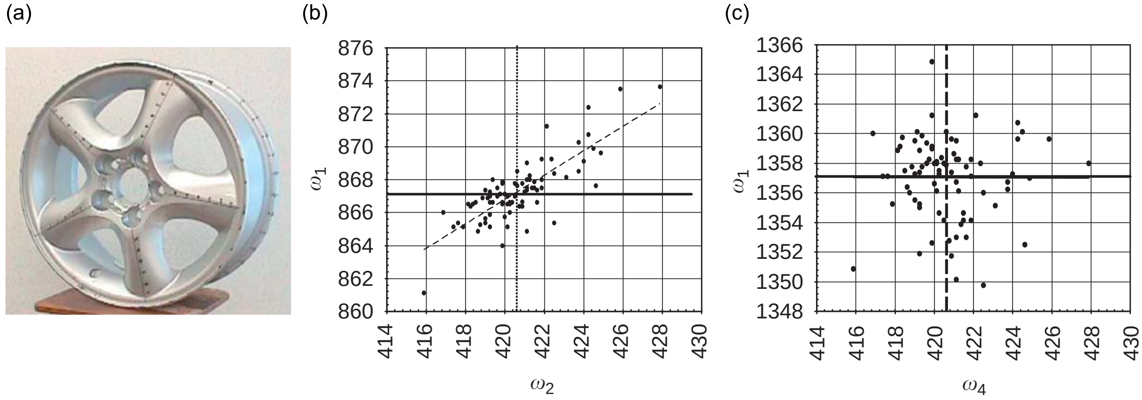

Fig. 2. (a) Alloy wheel rim and correlation between (b) first and second and (c) first and fourth natural frequencies.

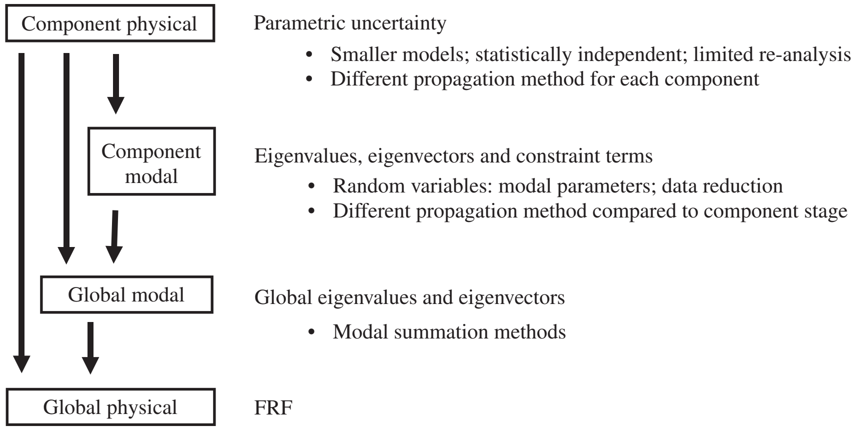

Fig. 3. Outline of uncertainty propagation in CMS.

process as being normally distributed and independent, although the measured correlation could of course be included. Neglecting this would be an approximation. Of course, determining the mode shapes and their statistics would be very difficult.

3.2. Uncertainty propagation

There are a number of different paths of uncertainty propagation as indicated in Fig. 3. Propagation through each path might involve Monte Carlo simulation (MCS), perturbations, interval analysis or whatever. In a classical analysis, the variation in physical properties might be propagated directly to the global physical level, e.g. the frequency response function (FRF). In a modal approach, first the variations in global modal properties are calculated, which are subsequently propagated to the global physical level. Within the CMS framework, a further coordinate level is introduced. Therefore, a total of three different and independent propagation steps can be considered: propagation from component physical to component modal and thence to global modal and finally global response. This offers several advantages.

First, at the component level, only those components where uncertainty is significant have to be considered: reanalysis is not required for any deterministic components. Secondly, the size of each component model is much smaller than that of the original global problem and computational cost is therefore less. If components are considered to be statistically independent, as is usually the case since they are typically made by different manufacturing processes and then assembled, then the physical and modal properties of two components are uncorrelated. The number of random variables is also smaller. These make MCS, interval analysis etc. more attractive. A further advantage is that different propagation approaches—exact, approximate, MCS, perturbational, probabilistic or possibilistic—can be applied as appropriate to each component, with models synthesised at the global modal level. Hybrid probabilistic and possibilistic descriptions can be unified by putting bounds on the distributions of modal parameters. An example is considered below. It is well known that correlation between variables can lead to very conservative results in a possibilistic analysis—such interdependency, where it exists, should be taken into account (e.g. [21]). Finally, there are different strategies for non-deterministic modal superposition that can be applied to estimate the FRF and its statistics.

3.3. Perturbations, modal sensitivities and CMS

Perturbation methods can be used to replace numerically expensive operations, such as solving an eigenvalue problem. The propagation problem is then reduced to an algebraic equation, which makes MCS and interval methods relatively computationally cheap. The CMS framework is particularly amenable to the application of perturbation methods to the propagation of uncertainty through one or more of the paths from component physical to component modal properties or component modal to global modal properties. These would be aimed in particular at those paths where there is only weak nonlinearity between input and output. The computational cost is then very small, primarily involving the cost associated with the estimation of gradients. In this section, various applications of perturbation approaches within the CMS framework are presented.

The rate of change of an eigenvalue λ_i with respect to some parameter p_j is [22]

$$\frac{\partial \lambda_i}{\partial p_j} = \boldsymbol{\phi}_i^{\mathrm{T}} \left(\frac{\partial \mathbf{K}}{\partial p_j} - \lambda_i \frac{\partial \mathbf{M}}{\partial p_j} \right) \boldsymbol{\phi}_i \tag{20}$$

where $\mathbf{M}(\mathbf{p})$ and $\mathbf{K}(\mathbf{p})$ are the mass and stiffness matrices, respectively, functions of the parameter vector $\mathbf{p}$, and $\boldsymbol{\phi}_i$ is the ith eigenvector. The first-order sensitivity of the ith eigenvector with respect to parameter p_j is [22]

$$\frac{\partial \boldsymbol{\phi}_i}{\partial p} = -\frac{1}{2} \left(\boldsymbol{\phi}_i^{\mathrm{T}} \frac{\partial \mathbf{M}}{\partial p} \boldsymbol{\phi}_i \right) \boldsymbol{\phi}_i + \sum_{k=1, k \neq i}^{N} \frac{\boldsymbol{\phi}_k^{\mathrm{T}} (\partial \mathbf{K}/\partial p - \omega_i^2 \partial \mathbf{M}/\partial p) \boldsymbol{\phi}_i}{\omega_i^2 - \omega_k^2} \boldsymbol{\phi}_k \tag{21}$$

Expressions also exist for second-order perturbations [22].

In classical approaches, the perturbation of Eq. (20) can be used for propagation from component physical to global modal properties. In the CMS framework it describes either propagation from component physical to component modal properties, or from component modal to global modal properties, as described in the next two subsections.

3.3.1. Perturbation from physical to component modal properties

The baseline component modal properties are given by the deterministic solution and only the derivatives of the component stiffness and mass matrices with respect to the uncertain physical parameters p have to be obtained. If a sensitivity matrix $\mathbf{R}$ is defined such that $r_{ji} = \partial \lambda_i / \partial p_j$, the covariance matrix of the eigenvalues can be approximated from the covariance matrix of the physical parameters as

$$COV(\lambda) = \mathbf{R}\, COV(\mathbf{p}) \mathbf{R}^{\mathrm{T}} \tag{22}$$

In practice, spatially varying physical properties can be modelled by random fields [18]. In FE methods, these are discretised using the existing mesh. In this case, $\mathbf{p}$ is a vector of correlated FE properties and $COV(\mathbf{p})$ is the covariance matrix as used in the representation of random fields. The gradients r_{ji} depend on the FE model and their calculation might not be trivial. Note again that quantification of the correlation function and parameters of a random field might, in practice, be impossible.

3.3.2. Perturbation from component modal to global modal properties

The special structure of the global matrices in the fixed-interface CMS method (Eq. (12) or (17)), especially the fact that the component eigenvalues appear uncoupled on the diagonal of the stiffness matrix, has many advantages. One of them concerns the formulation of a local modal/perturbational propagation method [8] in CMS. The sensitivity of the global modal properties can be calculated using Eq. (20), where the uncertain parameters p_j are now the component eigenvalues λ_j^c. It follows that

$$\frac{\partial \lambda_i^{gl}}{\partial \lambda_j^c} = (\boldsymbol{\phi}_i^{gl})_j^2 \tag{23}$$

where λ_i^{gl} and λ_j^c are the ith global and jth component eigenvalue, respectively, and $(\boldsymbol{\phi}_i^{gl})_j$ is the jth element of the ith baseline global eigenvector. Thus changes in the component eigenvalues can be related to changes in the global eigenvalues. A sensitivity matrix $\mathbf{S}$ can be defined such that $s_{ji} = ((\boldsymbol{\phi}_i^{gl})_j)^2$. If the covariance matrix $COV(\lambda^c)$ of the component eigenvalues is known, the covariance matrix of the global eigenvalues can be estimated by

$$COV(\lambda^{gl}) = \mathbf{S}COV(\lambda^c)\mathbf{S}^{\mathrm{T}} \tag{24}$$

This sensitivity approach can be extended to the propagation of uncertainties in the component and constraint mode shapes, but is less straightforward since these submatrices are not diagonal. The constraint mode shapes in particular seem to affect the FRF variability primarily for the lowest few modes, where the "static" terms are more important. A deviatoric component mode approach was suggested by De Gersem et al. [23] (see also De Gersem [24]), although quantifying the uncertainty in a practical situation is likely to be very difficult at best.

3.3.3. Perturbation between fixed and free-interface component modal properties

It is usually preferable to take experimental measurements of components in a free configuration which can be realised easily. For numerical analysis, however, fixed-interface (Craig–Bampton) methods are preferable for various reasons. Sensitivities relating the fixed and free-interface component modal properties can be used for a transformation between the coordinate systems. Consider a component with mass and stiffness matrices $\mathbf{m}$ and $\mathbf{k}$ in free configuration. The free-interface eigenvalues λ_i^{fr} can be found by solving the eigenvalue problem

$$(\mathbf{k} - \lambda_i^{fr}\mathbf{m})\boldsymbol{\phi}_i^{fr} = 0 \tag{25}$$

If there are fixed-interface conditions, the fixed-interface eigenvalues can be calculated from the eigenvalue problem of Eq. (3). Introducing the transformation defined by Eqs. (7) and (9), the eigenvalue problem

$$(\boldsymbol{\kappa} - \lambda_i^{fr}\boldsymbol{\mu})\boldsymbol{\phi}_i^{fr} = 0 \tag{26}$$

yields the free-interface eigenvalues λ^{fr}. Therefore, the free-interface eigenvalues depend on the fixed-interface eigenvalues and the constraint stiffness and mass terms in the matrices $\boldsymbol{\kappa}$ and $\boldsymbol{\mu}$. The derivative of the ith free-interface eigenvalue with respect to the jth fixed-interface eigenvalue is given by elements of the free-interface eigenvectors in the form

$$\frac{\partial \lambda_i^{fr}}{\partial \lambda_j^{fi}} = ((\boldsymbol{\phi}_i^{fr})_j)^2 \tag{27}$$

A sensitivity matrix $\mathbf{T}$, where $t_{ji} = ((\boldsymbol{\phi}_i^{fr})_j)^2$, can be used to estimate the covariance matrix of the free-interface eigenvalues from the covariance matrix of the fixed-interface eigenvalues by

$$COV(\lambda^{fr}) = \mathbf{T}COV(\lambda^c)\mathbf{T}^{\mathrm{T}} \tag{28}$$

In practice, it might be preferable, and much simpler, to quantify free-interface statistics of eigenvalues experimentally, while fixed-interface statistics are often preferred in a numerical analysis. These are related by

$$COV(\lambda^c) = \mathbf{T}^{-1}COV(\lambda^{fr})\mathbf{T}^{-\mathrm{T}} \tag{29}$$

Since the sensitivities relating the fixed and free-interface component modal properties depend also on constraint (or attachment) modes, for which experimental data might not be available, they are thus approximations.

4. Numerical examples

4.1. Uncertainties in components: two coupled beams

The first, illustrative example is the two-beam structure shown in Fig. 4. The components are rigidly connected to each other and clamped at the ends. The structure is modelled using standard FE matrices for Euler–Bernoulli beam theory [1], including transverse and rotational dofs. Each beam has bending stiffness EI, length L and mass per unit length ρA and is modelled by 10 elements (18 dofs per beam plus 2 interface dofs). The baseline values are given in Table 1. Damping is included by a modal loss factor of 3 percent. A fixed-interface CMS model is constructed and component normal modes corresponding to a frequency higher than 150 Hz are neglected. The accelerance FRF between two points, each 0.4 m from the clamped ends, will be considered. Uncertainty is introduced in the thickness h and Young's modulus E by a one-dimensional homogenous Gaussian random field model. The mean value is the baseline value, the coefficient of variance is 5 percent and the correlation length is 0.5 m for both variables. The continuous random field is discretised using the FE mesh.

4.1.1. Approximation considering variation in component eigenvalues only

A Monte Carlo approach with 1000 runs was applied in order to estimate eigenfrequency and FRF statistics. In addition to the exact solution, two approximate analyses are performed. First, variation is considered only in the global CMS stiffness matrix $\mathbf{K}$ (Eq. (12)) using the baseline constraint mass matrix $\mathbf{M}$. Second, variation is considered only in component eigenvalues $\mathbf{\Lambda}_{kk}$ using the baseline constraint mass and stiffness matrices. In Fig. 5, the errors in the estimated standard deviation of the global eigenfrequencies are shown. There are large relative differences for the first two eigenfrequencies, although absolute errors are small. Errors reduce for higher modes. In Fig. 6, the 5 and 95 percentiles of the magnitude of the FRFs are shown for the exact solution and the approximation considering variation only in the component eigenvalues. The agreement is good.

4.1.2. Combined probabilistic/possibilistic approach

In some circumstances it might be natural to describe the uncertainty in one component probabilistically, while the variation in another component is given by an interval. A hybrid approach might then be used by selecting the most appropriate propagation method—probabilistic or possibilistic—at the component level and unifying the uncertain data for the propagation to the global level. Of course this raises philosophical difficulties concerning the different treatments applied to different components, as well as practical issues relating to overestimation in the interval analysis, dependency of random variables and so on. Here it is suggested that probabilistic data is truncated at some appropriate level—in the examples at the 5 and

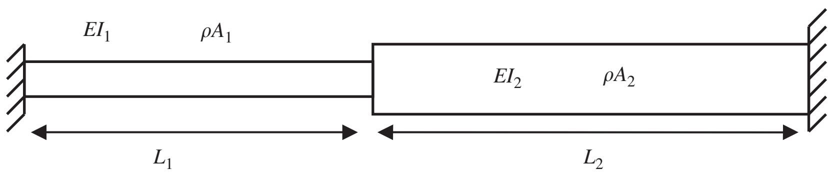

Fig. 4. Two coupled beams.

Table 1
Properties of two-beam example.

Component	L (m)	h (m)	b (m)	E (N/m^2)	ρ (kg/m^3)	$I = \frac{bh^3}{12}$
1	1	0.01	0.1	1e8	1000	$A = bh$
2	1	0.015	0.1	1e8	1000	

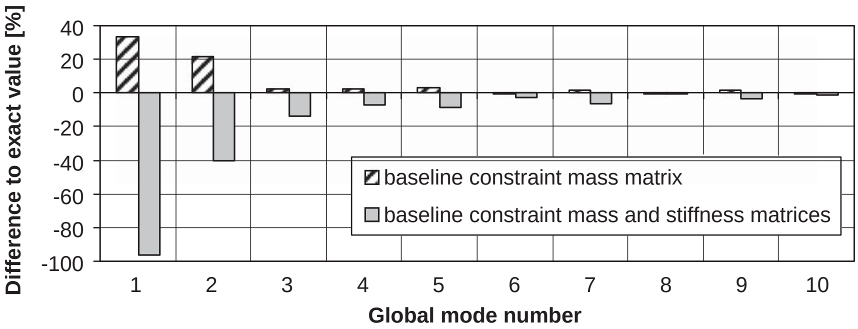

Fig. 5. Errors in estimated standard deviation of the global eigenfrequencies.

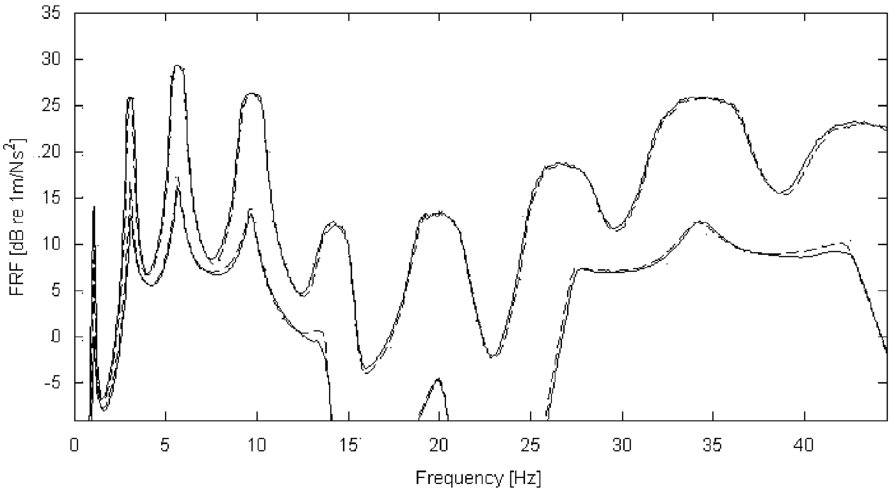

Fig. 6. FRF statistics, 5 and 95 percentiles of FRF magnitude: ____ exact solution and _ _ _ variation considered in component eigenvalues only.

95 percentiles—and thereafter treated as an interval quantity to give a global description in possibilistic terms. (Of course such bounds are not then strict bounds.)

In the CMS analysis, the 5 and 95 percentiles of the component eigenvalues are estimated first using MCS with 1000 runs. Second, an interval propagation approach to the global modal level is performed using the percentiles as lower and upper bounds. Finally, an FRF envelope is estimated based on the intervals on the global modal properties using the method described in [2]. The results of this hybrid sampling/interval approach are shown in Fig. 7. For comparison, the result of a classical interval analysis, starting at the physical level, is also shown. In the latter case, the 5 and 95 percentiles of the physical parameter distributions are used as lower and upper bounds and a uniform variation over all elements is assumed. An ensemble of 200 FRFs from a sampling approach based on the random field model is also shown. It can be seen that the hybrid method gives much closer bounds to the FRF than the classical interval approach. Therefore conservatism can be reduced if a sampling approach is adopted at component level.

4.1.3. Perturbational approach

Various perturbational approaches were suggested for the propagation of uncertainties. Eq. (22) can be used to estimate the covariance matrices of the component eigenvalues from the covariance matrices of uncertain physical parameters, such as those of a random field. Subsequently, Eq. (24) can be used to estimate the covariance matrix of the global eigenvalues. The corresponding first-order sensitivities for both relations are obtained from the baseline solution.

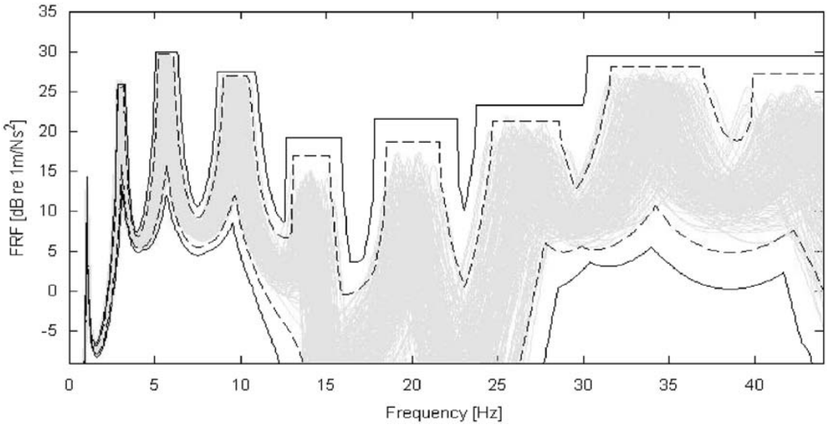

Fig. 7. FRF envelopes: ____ interval approach and _ _ _ hybrid sampling/interval approach.

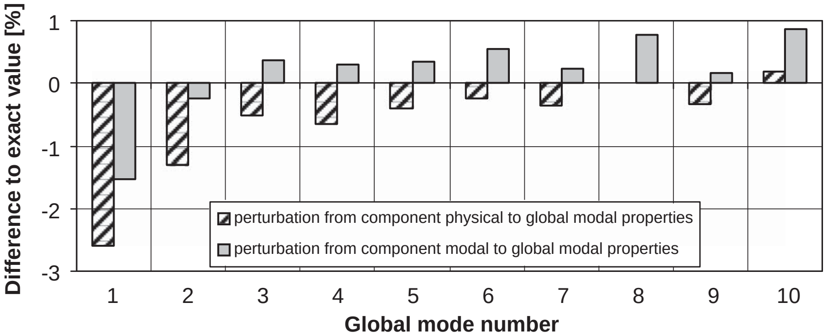

Fig. 8. Errors in standard deviation of the global eigenvalues due to perturbations.

In Fig. 8, the errors in the estimated standard deviations of the first 10 global eigenvalues are shown using two perturbation methods. In one, perturbations are applied to both propagation steps, i.e. from component physical to component modal and then to global modal properties. In the other case, perturbation is only considered for the propagation from component modal to global modal properties. The maximum error is 2.5 percent for the first two modes and less than 1 percent for the others. This accuracy is very satisfactory, especially in the context of other inaccuracies in analysis and quantification, and the level of uncertainty in general.

4.2. Uncertainties in joints: two coupled plates

As a second example consider the system comprising two plates shown in Fig. 9. In this case the interface dofs are reduced using CC modes. The plates are clamped on one edge and joined at the opposite edge. The stiffness of the line-coupling is uncertain and might represent a glue joint with a spatially varying stiffness, for example. Here the Young's modulus is modelled by a random field with a continuous exponential correlation function

$$f_R(r;\sigma,a) = \sigma^2 \exp\left(-\left|\frac{r}{a}\right|\right) \tag{30}$$

where r is the distance between two points, a the correlation length and σ the standard deviation. This is discretised on the FE mesh to yield the covariance matrix (c.f. $COV(\mathbf{p})$ in Eq. (22)). The plates are discretised using a mesh of 10×5 and 8×5 thin isotropic elements and the joint is modelled by six equidistant elastic elements. The baseline properties are given in Table 2.

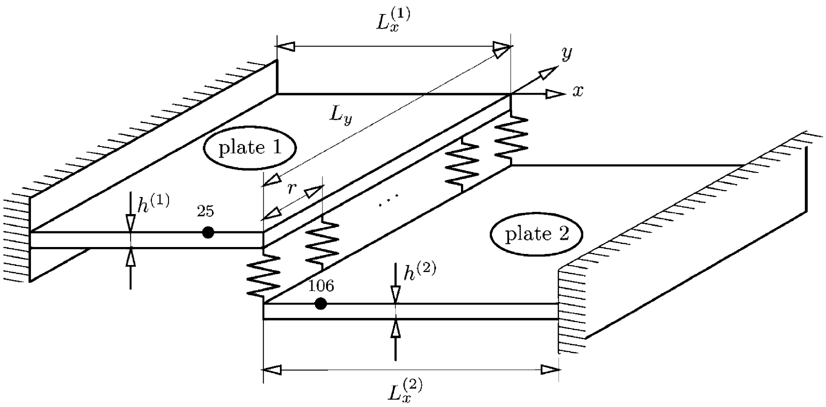

Fig. 9. Two line-coupled plates.

Table 2
Two coupled plates: baseline properties.

	Plate 1	Plate 2	Coupling	Units
ρ	2700	2700	1350	kg/m^3
E	7×10^7	7×10^7	3.5	kN/m^2
			35	
			70	
ν	0.3	0.3	–	–
L_x	$0.5\sqrt{2}$	0.5	0.006	m
L_y	0.5	0.5	0.5	m
h	3	3	3	mm
N_x	10	8	1	–
N_y	5	5	5	–

The response and its statistics depend on the relative values of the dynamic stiffnesses of the plates and the joint in the frequency range of interest (three different values are considered), the amount of uncertainty, the correlation length, whether the mode is predominantly bending or twisting and so on.

Three different values for the coupling elastic modulus E_c are considered. For the case where the elastic modulus of the coupling is 35 kPa the input and transfer mobilities are shown in Figs. 10(a) and (b) (see Fig. 9 for reference points). Results for the full solution of the multi degree of freedom model (mdof), the fixed-interface model (Eq. (11), CB) and the model with CC modes (Eq. (15), CBCC) are shown. The accuracies of the reduced models are such that their predictions are virtually indistinguishable from those of the full model, except around a few antiresonances. The relative calculation times are summarised in Table 3, illustrating the reduction of computational cost arising from the use of CMS. The accuracy is very good especially in the vicinity of resonances, less so in the vicinity of antiresonances, when the effects of neglected modes becomes relatively more important. The cost and accuracy depend of course on the number of kept interior and interface coordinates.

The sensitivities of the natural frequencies and mode shapes with respect to the elastic modulus of the coupling element are shown in Fig. 10(c). The sensitivity of the natural frequency follows from Eq. (20). If the sensitivity of the natural frequency to uncertainty is large the corresponding resonance frequency varies by a relatively large amount. The sensitivity of a mode shape to the uncertainty is defined in a manner analogous to the modal assurance criterion (MAC [25]) angle θ_j as

$$MAC = \cos^2\theta_j = \frac{(\boldsymbol{\phi}_j^{\mathrm{T}}\mathbf{W}\hat{\boldsymbol{\phi}}_j)^2}{(\hat{\boldsymbol{\phi}}_j^{\mathrm{T}}\mathbf{W}\hat{\boldsymbol{\phi}}_j)(\boldsymbol{\phi}_j^{\mathrm{T}}\mathbf{W}\boldsymbol{\phi}_j)}, \quad \hat{\boldsymbol{\phi}}_j = \boldsymbol{\phi}_j + \frac{\partial\hat{\boldsymbol{\phi}}_j}{\partial p}\Delta p \tag{31}$$

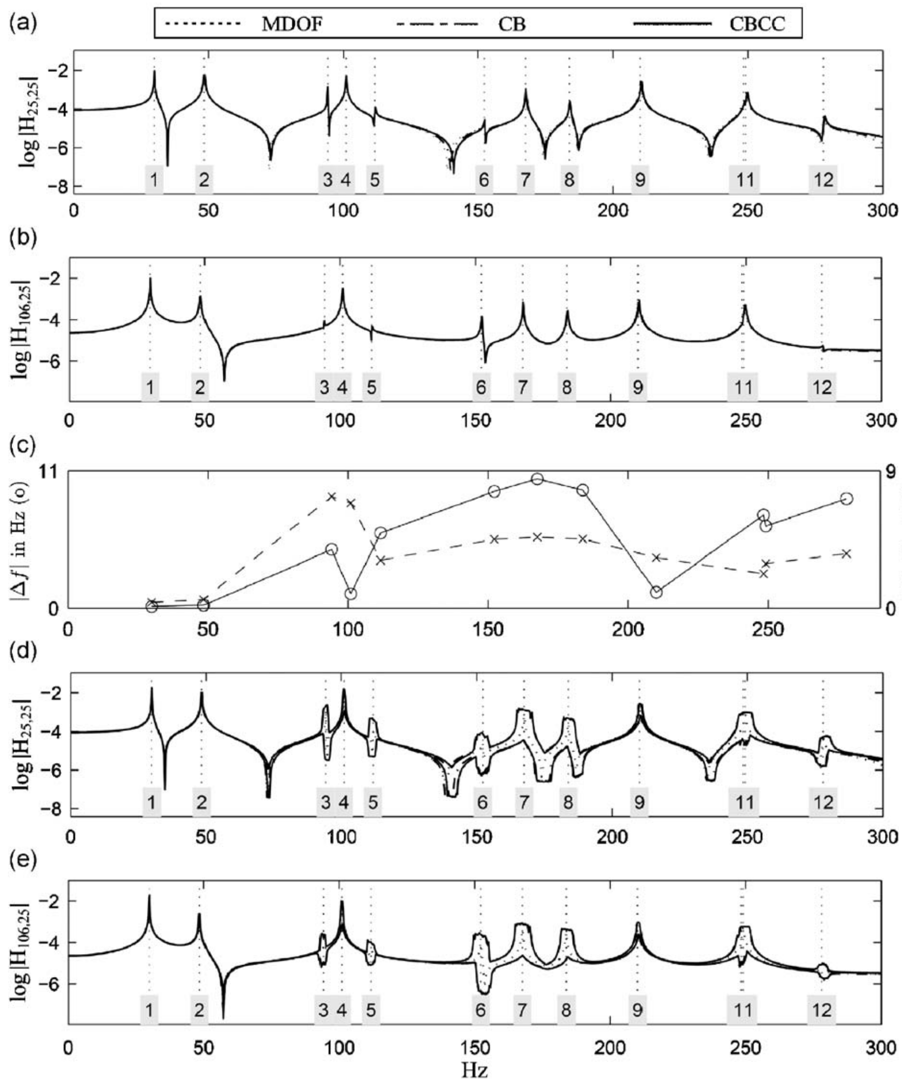

Fig. 10. Mobilities of 2-plate system with uncertain joint, $E_c = 35\,\mathrm{kPa}$, $a = 0.001$.

Table 3
Two coupled plates: comparison of calculation times for baseline system at 1000 frequency points.

Model	Matrix size	Joint dofs	Time (%)
mdof	324	36	100
CB	66	36	3.1
CBCC	45	15	1.6

where $\mathbf{W}$ is a matrix of weights and Δp the measure of the uncertainty (perhaps the standard deviation for a probabilistic parameter or half the size of the interval for one described possibilistically). Commonly, and in the example here, $\mathbf{W}$ is the mass matrix $\mathbf{M}$ of the structure, although the stiffness matrix $\mathbf{K}$ is occasionally used (or perhaps, if $\boldsymbol{\phi}_j$ contains a consistent set of dofs, the identity matrix). If mass normalised modes are used and the changes in the uncertain parameters are small then

$$\cos\theta_j \approx 1 + \boldsymbol{\phi}_j^{\mathrm{T}} \mathbf{W} \frac{\partial \hat{\boldsymbol{\phi}}_j}{\partial p} \Delta p \tag{32}$$

Larger values of the MAC angle lead to larger changes in the modal amplitudes, even if the resonance frequency is insensitive to joint uncertainty, since the response at resonance is typically dominated by the mode shape of the resonant mode. In the example shown the elastic modulus of each coupling element is normally distributed with a coefficient of variation equal to 6.6 percent and is truncated at levels of $\pm 3\sigma$, while $\Delta p = 3\sigma$. For this case the response statistics are relatively insensitive to modes 1, 2, 4 and 9.

Figs. 10(d) and (e) show results of MCS of the models CB and CBCC for a random field with small correlation length ($a = 0.001$, almost uncorrelated). The envelopes of the response are obtained from 1000 samples. Results using CB and CBCC are nearly the same except around some antiresonances, while response uncertainties are seen to be larger at frequencies around the more sensitive modes, as expected.

Fig. 11 shows FRF envelopes for the cases of weaker and stronger coupling, i.e. $E_c = 3.5$ and 70 kPa, together with the baseline solutions. Again, CB and CBCC approaches agree very well with full MCS on the mdof system, but at much reduced computational cost. The sensitivities of the individual natural frequencies and mode shapes depend on E_c and hence the FRF envelopes differ. For example, for stronger coupling the lower modes are barely affected by the joint uncertainty because the joint is relatively stiff compared to the dynamic stiffnesses of the plates. The natural frequencies of the weaker coupled system are smaller than those in Fig. 10, where $E_c = 35$ kPa, while those of the stronger coupled system are increased. Finally, results for a random field with a large correlation length $a = 1000$ are shown in Fig. 12.

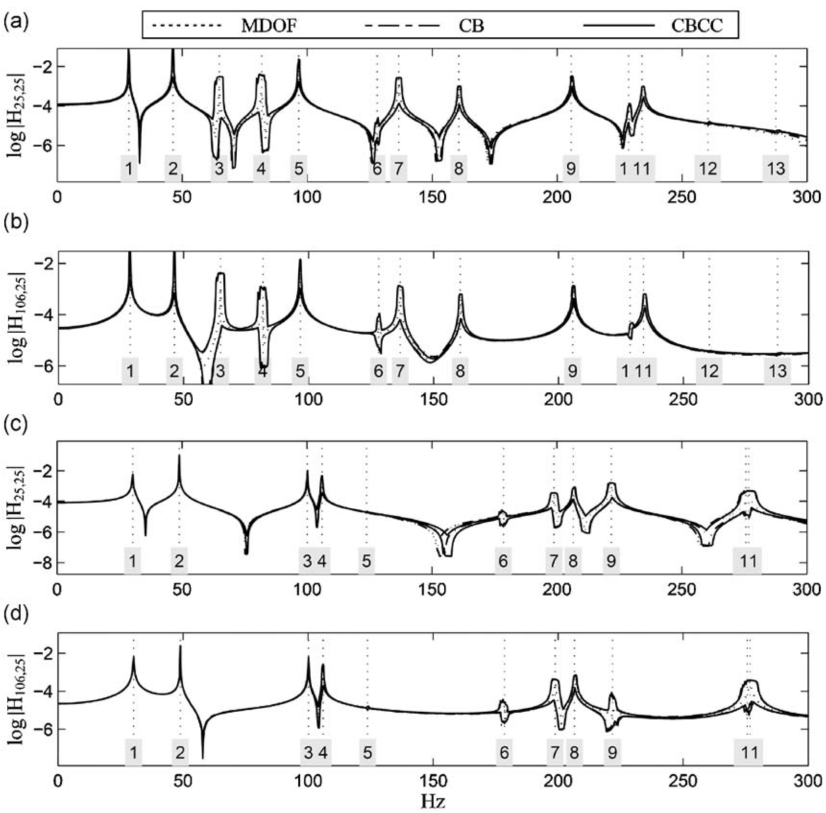

Fig. 11. Mobilities of 2-plate system with uncertain joint: (a) and (b) $E_c = 3.5$ kPa and (c) and (d) $E_c = 70$ kPa; $a = 0.001$.

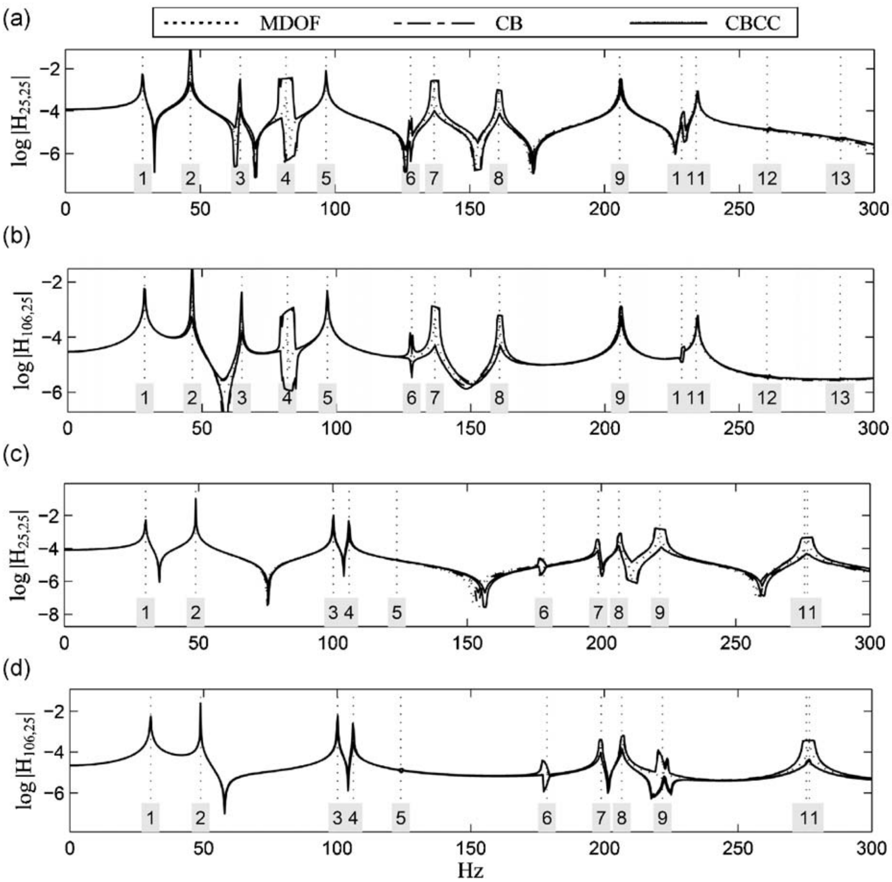

Fig. 12. Mobilities of 2-plate system with uncertain joint: (a) and (b) $E_c = 3.5\,\mathrm{kPa}$ and (c) and (d) $E_c = 70\,\mathrm{kPa}$; $a = 1000$.

5. Concluding remarks

Component mode synthesis is a well established method for the deterministic analysis of built-up structures. In particular, the implementation of fixed-interface CMS, perhaps with CC modes, is straightforward and systematic. CMS also provides an appealing framework for the analysis of structures with uncertain properties. Computational cost is reduced as a result of model reduction and this reduces the cost of multiple reanalysis as might be required in MCS, interval analysis and so on. There are further benefits, however.

Various advantages concerning uncertainty propagation accrue from the fact that CMS introduces a further level, the component modal level, in the description of the system and hence additional paths through which uncertainty propagates. The propagation of uncertainties from physical to component modal coordinates and from component modal to global modal coordinates can be treated independently. Deterministic components do not require reanalysis, while the propagation approach from component physical to component modal levels can be selected according to the nature and level of uncertainties existing in the component. This makes the use of perturbational methods in particular more widespread. Perturbational techniques are also applicable to the propagation from component modal to global modal levels—because the global mass and stiffness matrices possess a special structure the sensitivities in this step are already known from the solution to the baseline problem. These perturbations can be performed at very little cost.

There are also potential advantages regarding a reduction in uncertain variables at component modal level. For example, for the numerical propagation of uncertainties several benefits arise if the variations in the constraint terms, especially the off-diagonal terms, are neglected. However, this introduces approximation errors, particularly for the lower modes, as illustrated in the example in Section 4. For higher frequencies, the approximation gives good results. Other errors arise if the variations in the component modal matrices are neglected. Overall the approximation of considering uncertainty only in component eigenvalues seems reasonable for a frequency range where the lower limit is determined by the influence of the constraint terms. If this approximation is made, the analysis simplifies greatly. Finally, it is worth noting that the approximation errors introduced may well be comparable to errors in the quantification of uncertainty in the component physical properties.

The fact that CMS introduces a new level in the analysis, the component modal level, raises the possibility of quantification of uncertainty in terms of these component modal properties. In particular, quantifying the uncertainty in component eigenfrequencies experimentally is straightforward, for example from hammer tests. In practice such tests might be performed with a free rather than a fixed interface, but it is possible to estimate the statistics of one from the other. In contrast, it is much more difficult to quantify the variation in normal, constraint and CC modes experimentally, although the difficulties are no worse than quantifying the spatial variation of physical properties. It appears also that in many cases the response statistics are less sensitive to these properties, at least for higher modes.

A further strength of CMS is the ability to combine component models with qualitatively different uncertainty descriptions. In particular this might involve the combination of components described by both probabilistic and possibilistic data. In such a hybrid approach the different descriptions of uncertain properties can be considered at component level and then combined for the propagation to the global modal level.

Finally, uncertainty in damping has not been considered here. Assuming the damping is proportional and can be ascribed to the (undamped) modes, uncertainty mainly affects the magnitude of the FRF around resonances and antiresonances. This uncertainty can be included in the propagation path from global modes to FRFs, is independent of the eigenvalue and eigenvector analysis and involves little extra cost.

Acknowledgements

Part of this research has been carried out in the context of the European Marie Curie Research Training Network (MCRTN) "MADUSE" (Modelling Product Variability and Data Uncertainty in Structural Dynamics Engineering; www.maduse.org). The support of the European Commission is gratefully acknowledged.

References

[1] M. Petyt, *Introduction to Finite Element Vibration Analysis*, Cambridge University Press, Cambridge, 1990.
[2] D. Moens, D. Vandepitte, A survey of non-probabilistic uncertainty treatment in finite element analysis, *Computer Methods in Applied Mechanics and Engineering* 194 (2005) 1527–1555.
[3] G.I. Schuëller, Computational stochastic mechanics—recent advances, *Computers & Structures* 79 (2001) 2225–2234.
[4] W.C. Hurty, Dynamic analysis of structural systems using component modes, *AIAA Journal* 3 (1965) 678–685.
[5] R.R. Craig, M. Bampton Jr., Coupling of substructures for dynamic analysis, *AIAA Journal* 6 (1968) 1313–1319.
[6] R.B. Hintz, Analytical methods in component modal synthesis, *AIAA Journal* 13 (8) (1975) 1007–1016.
[7] R.R. Craig Jr., A review of time-domain and frequency-domain component mode synthesis methods, *Journal of Modal Analysis* 2 (2) (1987) 59–72.
[8] B.R. Mace, P.J. Shorter, A local modal/perturbational method for estimating frequency response statistics of built-up structures with uncertain properties, *Journal of Sound and Vibration* 242 (5) (2001) 793–811, Academic Press, New York.
[9] H. De Gersem, D. Moens, W. Desmet, D. Vandepitte, Interval and fuzzy dynamic analysis of finite element models with superelements, *Computers & Structures* 85 (2007) 304–319.
[10] O. Giannini, M. Hanss, The component mode transformation method: a fast implementation of fuzzy arithmetic for uncertainty management in structural dynamics, *Journal of Sound and Vibration* 311 (2008) 1340–1357.
[11] M.P. Castanier, Y.C. Tan, C. Pierre, Characteristic constraint modes for component mode synthesis, *AIAA Journal* 39 (6) (2001) 1182–1186.
[12] F. Bourquin, Component modal synthesis and eigenvalues of second-order operators: discretization and algorithm, *Mathematical Modelling and Numerical Analysis* 26 (3) (1992) 385–423.
[13] F. Bourquin, F. d'Hennezel, Numerical study of an intrinsic component mode synthesis method, *Computer Methods in Applied Mechanics and Engineering* 97 (1992) 49–76.

[14] K. Brahmi, N. Bouhaddi, R. Fillod, Reduction of the junction degrees of freedom before assembly in dynamic substructuring, *Design Engineering Technical Conferences*, ASME, Boston, USA, 1995.
[15] E. Balmes, Use of generalized interface degrees of freedom in component mode synthesis, *Proceedings of International Modal Analysis Conference*, 1996, pp. 204–210.
[16] D.-M. Tran, Component mode synthesis methods using interface modes. Application to structures with cyclic symmetry, *Computers & Structures* 79 (2001) 209–222.
[17] M. Guedri, N. Bouhaddi, R. Majed, Reduction of the stochastic finite element models using a robust dynamic condensation method, *Journal of Sound and Vibration* 297 (2006) 123–145.
[18] E. Vanmarcke, *Random Fields: Analysis and Synthesis*, MIT Press, Cambridge, MA, 1983.
[19] L. Hinke, B.R. Mace, T.P. Waters, Uncertainty quantification and CMS: free and fixed interface methodologies, *IMAC XXV*, Florida, 2006.
[20] R. Brown, J. Gear, *Dynamic Variations within Nominally Identical Product Lines*, Fourth year project, University of Auckland, September 1999.
[21] O. Giannini, M. Hanss, An interdependency index for the outputs of uncertain systems, *Fuzzy Sets and Systems* 159 (2008) 1292–1308.
[22] R.L. Fox, M.P. Kapoor, Rate of change of eigenvalues and eigenvectors, *AIAA Journal* 6 (12) (1968) 2426–2429.
[23] H. De Gersem, D. Moens, W. Desmet, D. Vandepitte, On the use of deviatoric component modes for the assessment of uncertainty in component mode synthesis, *First International Conference on Uncertainty in Structural Dynamics*, Sheffield, 2007.
[24] H. De Gersem, Interval Component Mode Synthesis Procedure for the Dynamic Analysis of Large FE Models, PhD Thesis, Katholieke Universiteit Leuven, 2008.
[25] D.J. Ewins, *Modal Testing: Theory, Practice and Applications*, second ed., Research Studies Press Ltd., New York, 2001.